



**NASA
Technical
Paper
3352**

August 1993

Coulomb Effects in Low-Energy Nuclear Fragmentation

John W. Wilson,
Sang Y. Chun,
Francis F. Badavi,
and Sarah John


**NASA
Technical
Paper
3352**

1993

Coulomb Effects in Low-Energy Nuclear Fragmentation

John W. Wilson,
*Langley Research Center
Hampton, Virginia*

Sang Y. Chun
*Old Dominion University
Norfolk, Virginia*

Francis F. Badavi
*Christopher Newport University
Newport News, Virginia*

Sarah John
*ViGYAN, Inc.
Hampton, Virginia*

Abstract

Early versions of the Langley nuclear fragmentation code NUCFRAG (and a publicly released version called HZEFRG1) assumed straight-line trajectories throughout the interaction. As a consequence, NUCFRAG and HZEFRG1 give unrealistic cross sections for large mass removal from the projectile and target at low energies. A correction for the distortion of the trajectory by the nuclear coulomb fields is used herein to derive fragmentation cross sections. A simple energy-loss term is applied to estimate the energy downshifts that greatly alter the coulomb trajectory at low energy. The results, which are far more realistic than prior versions of the code, should provide the data base for future transport calculations. The systematic behavior of charge-removal cross sections compares favorably with results from low-energy experiments.

Introduction

The cross sections in the radiation physics program at the Langley Research Center have a long history. Early transport calculations (ref. 1) were developed using the work of Waddington and coworkers (ref. 2) that was derived mainly from nuclear emulsion data obtained in high-altitude balloons. These cross sections were soon abandoned in favor of corrections to Rudstam's work (ref. 3) that were derived by Silberberg and Tsao (ref. 4) from radionuclide production data. The Silberberg-Tsao model was mainly appropriate for high charge and energy ions (HZE) fragmentation on hydrogen targets, although a modification of the scaling procedure of Lindstrom et al. (ref. 5) was used for arbitrary target nuclei (ref. 6). The cross sections of reference 6 were used to explain the Bragg curves of Ne beams in laboratory experiments (ref. 7). The scaled Silberberg-Tsao cross sections (augmented with Bertini (ref. 8) cross sections for the lightest fragments n , p , d , t , he , and α) significantly underestimated the experimental Bragg curves. The cause, in part, resulted from the lack of mass and charge conservation of the cross-section data set. Cross-section renormalization to ensure mass and charge conservation improved the agreement (ref. 7).

The next stage of transport development was based on a study of atmospheric air shower data (refs. 9 and 10). No agreement could be found with the charge 3–10 group as measured in the atmosphere because of the very large cross sections predicted by reference 6 for the production of Li, Be, and B by air nuclei from galactic cosmic rays incident at the top of the atmosphere (ref. 10). The production of a version of the model by Bowman, Swiatecki, and Tsang (ref. 11) was attempted with some improvement, but unsatisfactory agreement was found with the air shower data (ref. 10). At that point, the first version of the NUCFRAG model was derived

as a modification of reference 11, and good agreement was obtained with the air shower data (ref. 10). The NUCFRAG code calculates the average excitation from frictional forces at the interface of the interaction zone and an empirical correction to the surface energy for highly misshapened nuclei (ref. 10).

The frictional forces are derived from two-body collisional processes, and the corresponding excitation energy is a fluctuating variable. The average value used in reference 10 was replaced by a random variable in reference 12 and was assumed to fluctuate between its maximum and minimum values with equal probability. This procedure gave a satisfactory fit to the fragmentation data of Westfall et al. (ref. 13) and Heckman (ref. 14).

More recently, the matter densities were used to determine nuclear radii, the energy-dependent nuclear mean free path was added, and an improved fit of the value of empirical correction to the excitation energy was made with reasonable agreement with available measured fragmentation cross sections (ref. 15). Most of the data to which the model was compared were of relatively high energies of 0.9 to 2.1 GeV/amu. Indeed, the cross sections for fragmenting a projectile of mass A_P into a fragment A_F with charge Z_F showed relatively little dependence on energy (especially for light-fragment production (n , p , d , t , he , and α)) as seen in figure 1 for H_2O targets. (Note that the early versions did not calculate d , t , and he cross sections, which were added only recently.) This absence is especially disturbing because one would assume that the removal of 80 percent of the mass from an iron nucleus might require more energy than the kinetic energy of 25 MeV/amu. Obviously, three important factors are missing from the NUCFRAG and HZEFRG1 (a publicly released version of NUCFRAG) codes. First, the straight-line trajectories throughout the interaction assumed in NUCFRAG underestimate the closeness of approach

between the projectile and target. Second, the kinetic energy of the projectile is downshifted as energy is given up to release nucleons in the collision event. Third, energy conservation occurs in particle knockout processes, and this effect further modifies the trajectory. The first two factors will be addressed herein.

Theory

The essence of the NUCFRAG (and HZEFRG1) code is that the mass removal ΔA from a projectile of mass A_P by collision with a target of mass A_T is a function of the impact parameter b . The assumption of straight-line trajectories also makes the impact parameter the distance of closest approach. Swiatecki, Bowman, and Tsang (ref. 11) suggested that the cross section for removal of ΔA nucleons $\sigma(\Delta A)$ is given by

$$\sigma(\Delta A) = \pi \left\{ \left[b \left(\Delta A - \frac{1}{2} \right) \right]^2 - \left[b \left(\Delta A + \frac{1}{2} \right) \right]^2 \right\} \quad (1)$$

which has brought these simple concepts to usefulness. We maintain this relationship but no longer take b to be the distance of closest approach.

Coulomb Trajectories

The equations of motion in the nuclear coulomb field are given by energy conservation as

$$E_{\text{tot}} = \frac{1}{2} \mu \dot{r}^2 + \frac{\ell^2}{2 \mu r^2} + \frac{Z_P Z_T e^2}{r} \quad (2)$$

where E_{tot} is the total kinetic energy in the center of mass system at large relative distances, r is the relative distance between the charge centers with time derivative \dot{r} , μ is the reduced mass, ℓ is the angular momentum, Z_P and Z_T are the atomic numbers of the projectile and target nucleus, respectively, and e is the electric charge. (That is, $e^2 = 2 R_y a_o$, where R_y is the Rydberg constant and a_o is the Bohr radius.) The angular momentum is given as

$$\ell^2 = 2 \mu E_{\text{tot}} b^2 \quad (3)$$

The distance of closest approach is given by equation (2) for $\dot{r} = 0$ as

$$E_{\text{tot}} = \frac{E_{\text{tot}} b^2}{r^2} + \frac{Z_P Z_T e^2}{r} \quad (4)$$

which we write as

$$b^2 = r(r - r_m) \quad (5)$$

where

$$r_m = \frac{Z_P Z_T e^2}{E_{\text{tot}}} \quad (6)$$

Note that r_m is the distance of closest approach for zero impact parameter. We now take the distance of closest approach r calculated by NUCFRAG at a given ΔA and calculate the impact parameter. Thus, we extrapolate backward in time along the coulomb trajectory to the initial impact parameter b using equation (5). This calculated value of b is used in equation (1) to evaluate the cross section. Note that the effect of the coulomb trajectory is to move the separation at impact r to smaller impact parameters b and thus reduce the cross sections, especially at low energy.

Energy Downshift

A second correction to the trajectory calculation comes from the transfer of kinetic energy into binding energy in the release of particles from the projectile. (Obviously, energy is also lost in releasing particles from the target, which we do not yet calculate.) The total kinetic energy in passing through the reaction zone is reduced to

$$E_f = E_i - 10 \Delta A \quad (7)$$

by assuming that 10 MeV is the average binding energy. The kinetic energy used in the closest approach calculation is the average

$$E_{\text{tot}} = \frac{1}{2}(E_i + E_f) = E_i - \frac{1}{2}(10 \Delta A) \quad (8)$$

Obviously, E_{tot} as given by equation (8) is very crude and substantial improvements can be made. Isobaric fragmentation cross sections of the old NUCFRAG model are shown in figure 1, and the coulomb revised cross sections are shown in figure 2. (Note that the curves labeled as mass 0–5 are for the light fragments n , p , d , t , he , and α .) The aforementioned formalism greatly improves the nuclear data base, as can be seen by comparing figure 1(a) with figure 2(a), but it is relatively ineffective at the higher energies above 600 MeV/amu. (Compare fig. 1(d) with fig. 2(d).)

Comparison With Experiments

As a test of the formalism, in figures 3 and 4 we compare our theory with the experimental data obtained by references 16 and 17, respectively. Qualitative agreement is achieved for charge removal from projectiles of O and Kr, even at very low energies. This agreement can likely be improved if the interference of nuclear dissociation and coulomb phase

shifts is calculated. Clearly, transfer processes are important at these energies and are not represented in the current model. The large cross section for $\Delta Z = 0$ observed for the ^{16}O experiment in figure 3 is probably due to exchange contributions at these low energies.

The elemental cross sections for $^{16}\text{O} + ^{27}\text{Al}$ reactions are shown in figure 5 at low energies. The HZE fragmentation cross sections in figure 5(a) experience the greatest variation below 25 MeV/amu, an effect arising mainly by coulomb deflection. A somewhat weaker variation above 25 MeV/amu results from the varying mean free path of the two-body collision. The light-fragment-production cross sections show rather strong energy dependence below 200 MeV/amu, as seen in figure 5(b). The elemental cross sections for $^{16}\text{O} + ^{204}\text{Ti}$ are shown in figure 6. The much stronger energy dependence shown in comparison with that of the aluminum target in figure 5 is due to the much greater charge of the titanium target.

Increasing the projectile charge produces an even greater energy variation of the HZE fragmentation cross sections, as shown in figure 7. The HZE fragmentation cross sections show even greater energy dependence, especially for $\Delta Z = 0, 1$ and $\Delta Z > 20$. The nearly linear dependence of the $\Delta Z = 0, 1$ cross sections is due to the coulomb excitation of the giant dipole resonance and the resultant coulomb dissociation (ref. 18). The strong variations for $\Delta Z > 20$ are due to the coulomb distortion of the collision trajectory. In all cases, the effects are most easily observed in the light-fragment-production cross sections which are sensitive to small changes in fragment distributions caused by the large multiplicities of light fragments, especially for heavy projectiles.

Concluding Remarks

The nuclear fragmentation cross sections are improved by calculating the interaction along the classical coulomb trajectory. An energy-loss term that is proportional to the mass removed in fragmenting is used as a correction to the distance of closest approach. The results are physically more meaningful at low energy than the prior code NUCFRAG (and a publicly released version called HZEFRG1), but they approach the older results above 600 MeV/amu. Further improvements in estimating the effects of energy loss should improve the present approximation. The adequacy of the present cross sections at low energy must await further experimental comparisons.

Reasonable agreement is obtained with low-energy charge-removal cross sections.

NASA Langley Research Center
Hampton, VA 23681-0001
May 6, 1993

References

1. Wilson, John W.: *Analysis of the Theory of High-Energy Ion Transport*. NASA TN D-8381, 1977.
2. Cleghorn, T. F.; Freier, P. S.; and Waddington, C. J.: The Energy Dependence of the Fragmentation Parameters and Mean Free Paths of Cosmic-Ray Nuclei With $Z \geq 10$. *Canadian J. Phys.*, vol. 46, no. 10, May 1968, pp. S572-S577.
3. Rudstam, G.: Systematics of Spallation Yields. *Zeitschrift fur Naturforschung*, vol. 21a, no. 7, July 1966, pp. 1027-1041.
4. Silberberg, R.; and Tsao, C. H.: Partial Cross-Sections in High-Energy Nuclear Reactions, and Astrophysical Applications. I. Targets With $Z \leq 28$. *Astrophys. J. Suppl. Ser.*, no. 220(I), vol. 25, 1973, pp. 315-333.
5. Lindstrom, P. J.; Greiner, D. E.; Heckman, H. H.; Cork, Bruce; and Bieser, F. S.: *Isotope Production Cross Sections From the Fragmentation of ^{16}O and ^{12}C at Relativistic Energies*. LBL-3650, Lawrence Berkeley Lab., Univ. of California, June 1975.
6. Silberberg, R.; Tsao, C. H.; and Shapiro, M. M.: Semi-empirical Cross Sections, and Applications to Nuclear Interactions of Cosmic Rays. *Spallation Nuclear Reactions and Their Applications*, B. S. P. Shen and M. Merker, eds., D. Reidel Publ. Co., c.1976, pp. 49-81.
7. Wilson, John W.; Townsend, L. W.; Bidasaria, H. B.; Schimmerling, Walter; Wong, Mervyn; and Howard, Jerry: ^{20}Ne Depth-Dose Relations in Water. *Health Phys.*, vol. 46, no. 5, May 1984, pp. 1101-1111.
8. Bertini, Hugo W.; Guthrie, Miriam P.; and Culkowski, Arline H.: *Nonelastic Interactions of Nucleons and π -Mesons With Complex Nuclei at Energies Below 3 GeV*. ORNL-TM-3148, U.S. Atomic Energy Commission, Mar. 28, 1972.
9. Wilson, John W.; and Badavi, F. F.: Methods of Galactic Heavy Ion Transport. *Radiat. Res.*, vol. 108, 1986, pp. 231-237.
10. Wilson, John W.; Townsend, Lawrence W.; and Badavi, Forooz F.: Galactic HZE Propagation Through the Earth's Atmosphere. *Radiat. Res.*, vol. 109, no. 2, Feb. 1987, pp. 173-183.
11. Bowman, J. D.; Swiatecki, W. J.; and Tsang, C. F.: *Ablation and Ablation of Heavy Ions*. LBL-2908, Lawrence Berkeley Lab., Univ. of California, July 1973.
12. Wilson, John W.; Townsend, Lawrence W.; and Badavi, F. F.: A Semiempirical Nuclear Fragmentation Model. *Nucl. Instrum. & Methods Phys. Res.*, vol. B18, no. 3, Feb. 1987, pp. 225-231.

13. Westfall, G. D.; Wilson, Lance W.; Lindstrom, P. J.; Crawford, H. J.; Greiner, D. E.; and Heckman, H. H.: Fragmentation of Relativistic ^{56}Fe . *Phys. Review*, ser. C, vol. 19, no. 4, Apr. 1979, pp. 1309–1323.
14. Heckman, H. H.: *Heavy Ion Fragmentation Experiments at the Bevatron*. NASA CR-142589, 1975.
15. Townsend, Lawrence W.; Wilson, John W.; Tripathi, Ram K.; Norbury, John W.; Badavi, Francis F.; and Khan, Ferdous: *HZEFRG1: An Energy-Dependent Semi-empirical Nuclear Fragmentation Model*. NASA TP-3310, 1993.
16. Lefort, Marc: Mass Distribution in Dissipative Reactions. The Frontier Between Fusion and Deep Inelastic Transfers. *Deep-Inelastic and Fusion Reactions With Heavy Ions*, W. von Oertzen, ed., *Volume 117 of Lecture Notes in Physics*, Springer-Verlag, 1980, pp. 25–42.
17. Lynen, U.: A Fast Splitting of Projectile-Like Fragments in the Reaction $^{86}\text{Kr}-^{166}\text{Er}$ at 12.1 MeV/u. *Deep-Inelastic and Fusion Reactions With Heavy Ions*, W. von Oertzen, ed., *Volume 117 of Lecture Notes in Physics*, Springer-Verlag, 1980, pp. 91–99.
18. Norbury, John W.; Townsend, Lawrence W.; and Badavi, Forooz F.: *Computer Program for Parameterization of Nucleus-Nucleus Electromagnetic Dissociation Cross Sections*. NASA TM-4038, 1988.

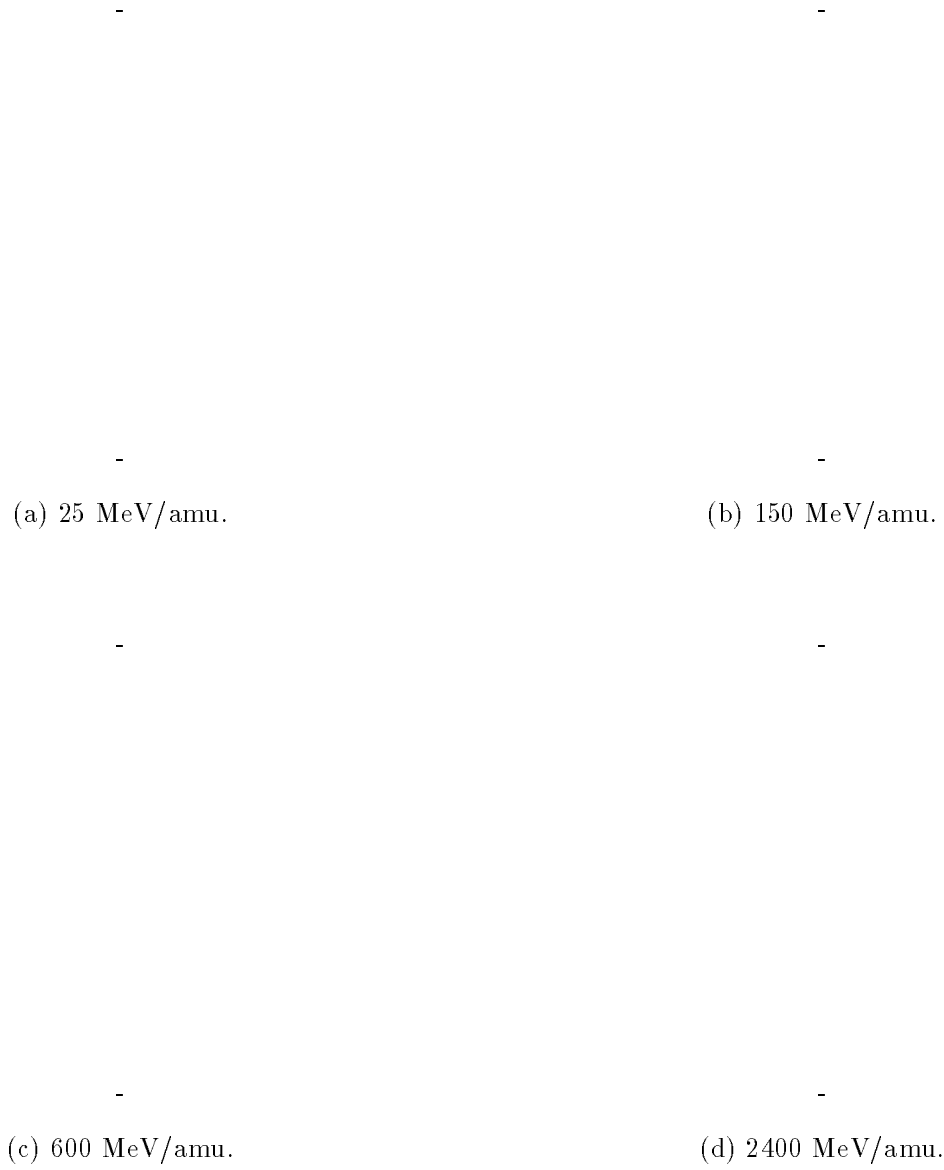


Figure 1. NUCFRAG cross sections in water for projectiles ${}^6\text{Li}$ through ${}^{59}\text{Ni}$ at various energies.

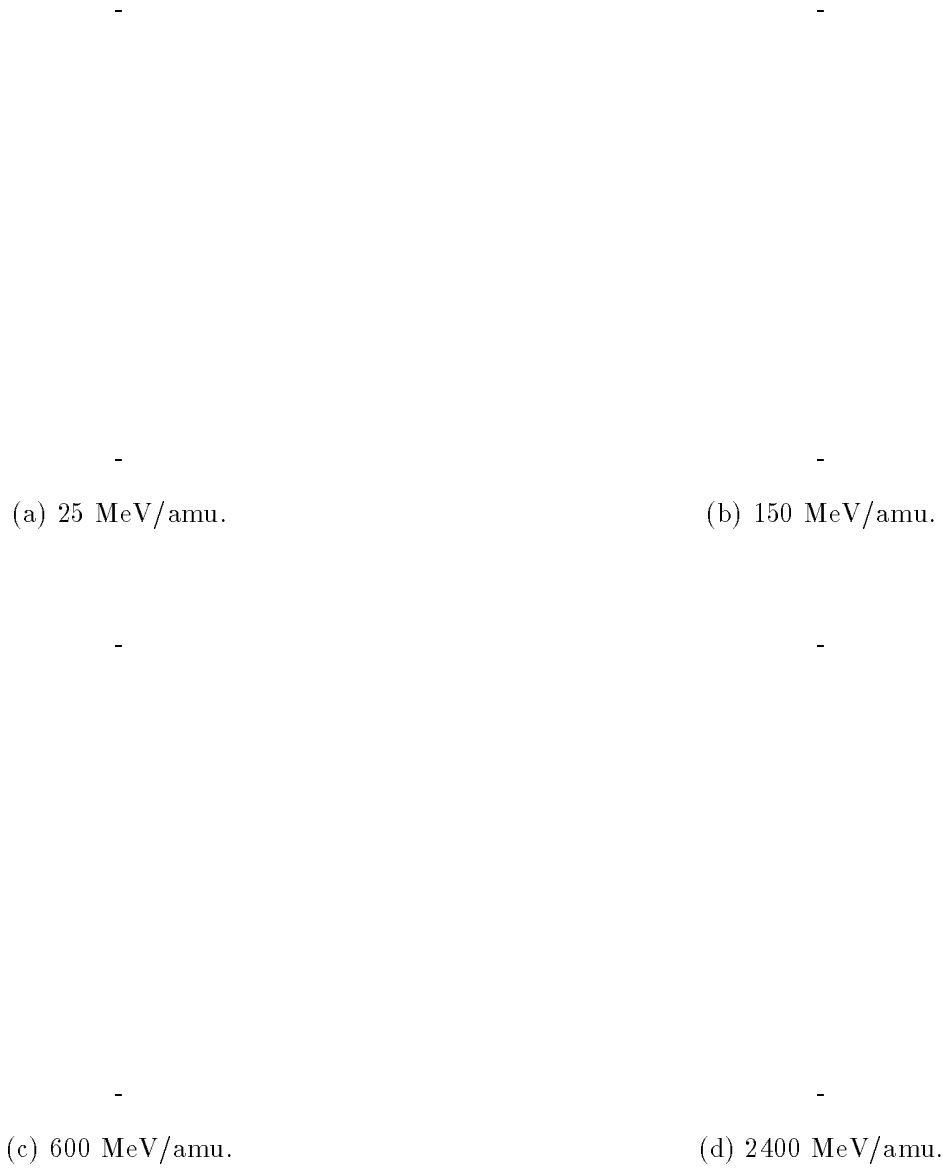


Figure 2. Coulomb revised cross sections in water for projectiles of ${}^6\text{Li}$ to ${}^{59}\text{Ni}$ at various energies.

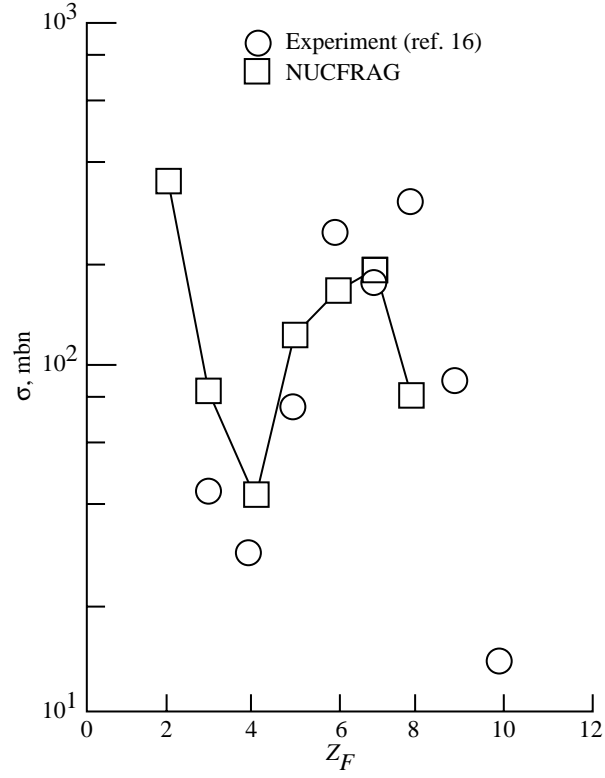


Figure 3. Charge-removal cross sections for 11.7 MeV/amu ^{16}O projectiles onto ^{92}Mo targets are shown with experimental values obtained by reference 16.

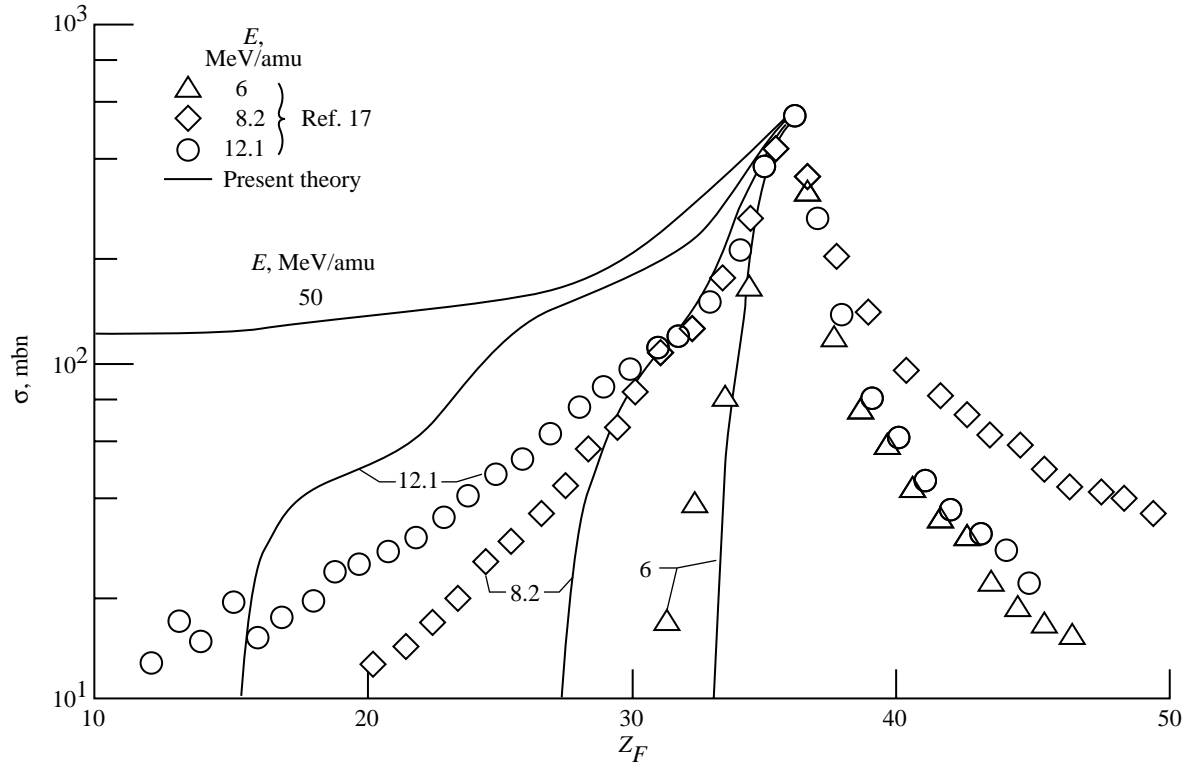
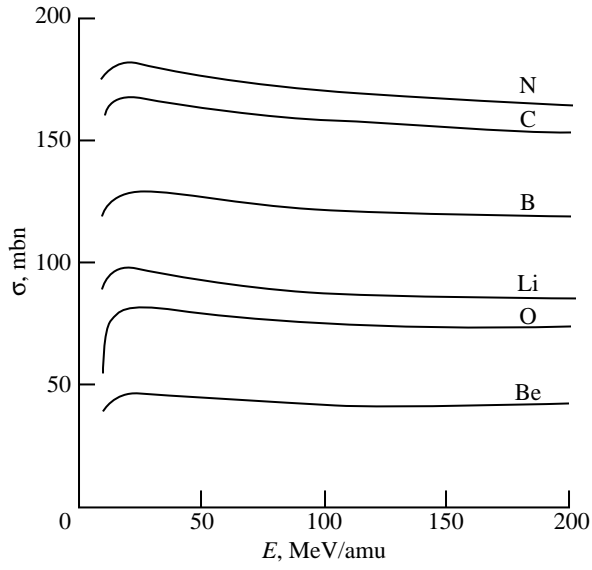
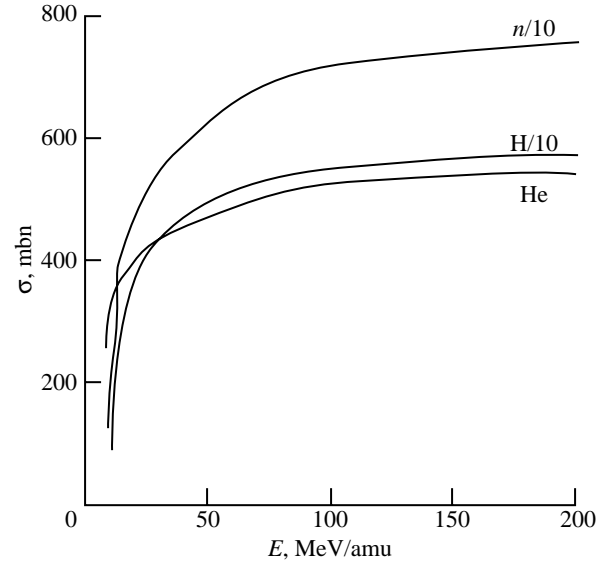


Figure 4. Charge-removal cross sections for ^{84}Kr projectiles onto ^{166}Er targets are shown with experimental values obtained by reference 17.

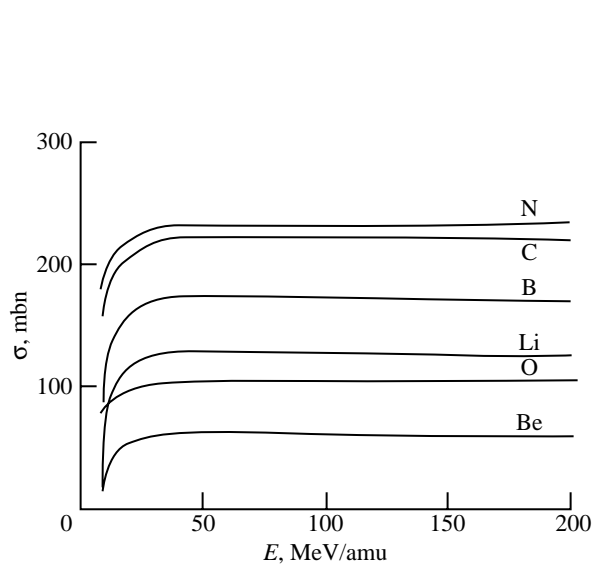


(a) HZE fragmentation.

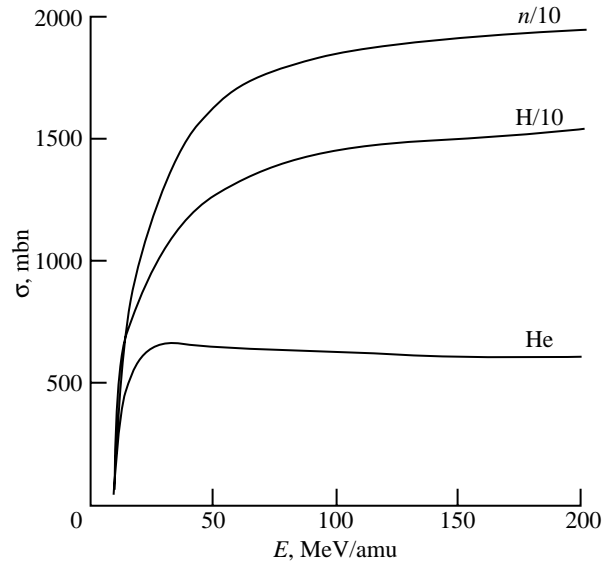


(b) Light fragment production.

Figure 5. Elemental cross sections for ^{16}O fragmentation on an aluminum target.

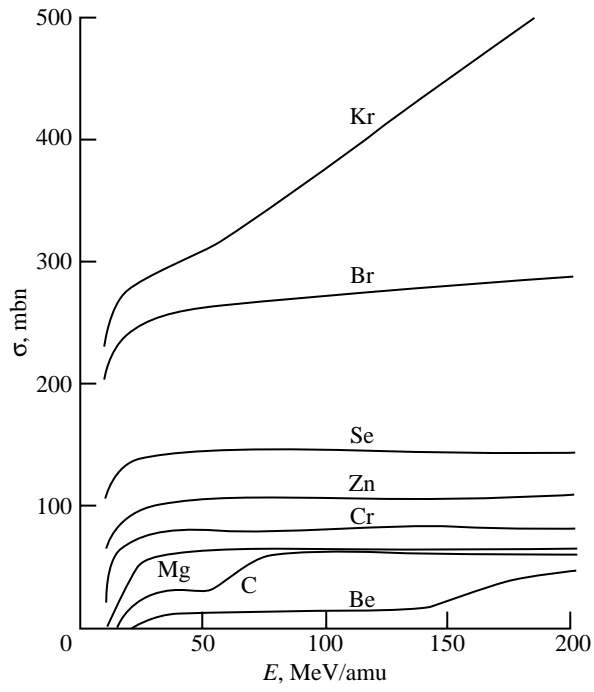


(a) HZE fragmentation.

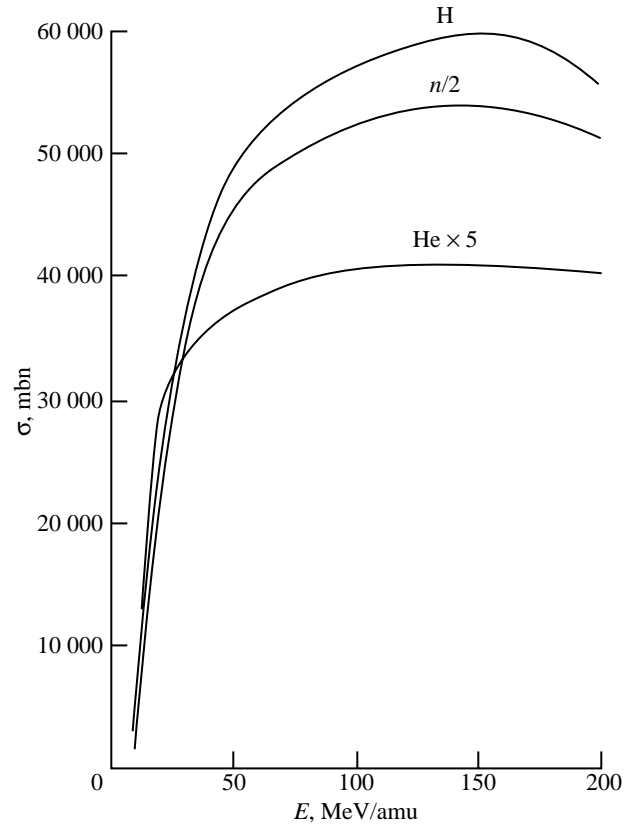


(b) Light fragment production.

Figure 6. Elemental cross sections for ^{16}O fragmentation on a titanium target.



(a) HZE fragmentation.



(b) Light fragment production.

Figure 7. Elemental cross sections for ^{84}Kr fragmentation on a titanium target.

- (a) 25 MeV/amu.
- (b) 150 MeV/amu.
- (c) 600 MeV/amu.
- (d) 2400 MeV/amu.

Figure 1. NUCFRAG cross sections in water for projectiles ${}^6\text{Li}$ through ${}^{59}\text{Ni}$ at various energies.

- (a) 25 MeV/amu.
- (b) 150 MeV/amu.
- (c) 600 MeV/amu.
- (d) 2400 MeV/amu.

Figure 2. Revised cross sections in water for projectiles of ${}^6\text{Li}$ to ${}^{59}\text{Ni}$ at various energies.

Figure 3. Charge-removal cross sections for 11.7 MeV/amu ${}^{16}\text{O}$ projectiles onto ${}^{92}\text{Mo}$ targets are shown with experimental values obtained by reference 16.

Figure 4. Charge-removal cross sections for ${}^{84}\text{Kr}$ onto ${}^{166}\text{Er}$ targets are shown with experimental values obtained by reference 17.

- (a) HZE fragmentation.
- (b) Light fragment production.

Figure 5. Elemental cross sections for ${}^{16}\text{O}$ fragmentation on an aluminum target.

- (a) HZE fragmentation.
- (b) Light fragment production.

Figure 6. Elemental cross sections for ${}^{16}\text{O}$ fragmentation on a titanium target.

- (a) HZE fragmentation.
- (b) Light fragment production.

Figure 7. Elemental cross sections for ${}^{84}\text{Kr}$ fragmentation on a titanium target.

REPORT DOCUMENTATION PAGE			Form Approved OMB No. 0704-0188	
Public reporting burden for this collection of information is estimated to average 1 hour per response, including the time for reviewing instructions, searching existing data sources, gathering and maintaining the data needed, and completing and reviewing the collection of information. Send comments regarding this burden estimate or any other aspect of this collection of information, including suggestions for reducing this burden, to Washington Headquarters Services, Directorate for Information Operations and Reports, 1215 Jefferson Davis Highway, Suite 1204, Arlington, VA 22202-4302, and to the Office of Management and Budget, Paperwork Reduction Project (0704-0188), Washington, DC 20503.				
1. AGENCY USE ONLY (Leave blank)		2. REPORT DATE August 1993		3. REPORT TYPE AND DATES COVERED Technical Paper
4. TITLE AND SUBTITLE Coulomb Effects in Low-Energy Nuclear Fragmentation			5. FUNDING NUMBERS WU 199-45-16-11	
6. AUTHOR(S) John W. Wilson, Sang Y. Chun, Francis F. Badavi, and Sarah John				
7. PERFORMING ORGANIZATION NAME(S) AND ADDRESS(ES) NASA Langley Research Center Hampton, VA 23681-0001			8. PERFORMING ORGANIZATION REPORT NUMBER L-17226	
9. SPONSORING/MONITORING AGENCY NAME(S) AND ADDRESS(ES) National Aeronautics and Space Administration Washington, DC 20546-0001			10. SPONSORING/MONITORING AGENCY REPORT NUMBER NASA TP-3352	
11. SUPPLEMENTARY NOTES Wilson: Langley Research Center, Hampton, VA; Chun: Old Dominion University, Norfolk, VA; Badavi: Christopher Newport University, Newport News, VA; John: ViGYAN, Inc., Hampton, VA.				
12a. DISTRIBUTION/AVAILABILITY STATEMENT Unclassified-Unlimited Subject Category 93			12b. DISTRIBUTION CODE	
13. ABSTRACT (Maximum 200 words) Early versions of the Langley nuclear fragmentation code NUCFRAG (and a publicly released version called HZEFRG1) assumed straight-line trajectories throughout the interaction. As a consequence, NUCFRAG and HZEFRG1 give unrealistic cross sections for large mass removal from the projectile and target at low energies. A correction for the distortion of the trajectory by the nuclear coulomb fields is used herein to derive fragmentation cross sections. A simple energy-loss term is applied to estimate the energy downshifts that greatly alter the coulomb trajectory at low energy. The results, which are far more realistic than prior versions of the code, should provide the data base for future transport calculations. The systematic behavior of charge-removal cross sections compares favorably with results from low-energy experiments.				
14. SUBJECT TERMS Nuclear fragmentation; Coulomb trajectory; Space radiation			15. NUMBER OF PAGES 10	
			16. PRICE CODE A02	
17. SECURITY CLASSIFICATION OF REPORT Unclassified	18. SECURITY CLASSIFICATION OF THIS PAGE Unclassified	19. SECURITY CLASSIFICATION OF ABSTRACT	20. LIMITATION OF ABSTRACT	